

# Electronic Supplementary Material

## Halide-free carbonylation of methanol with H-MOR supported CuCeO<sub>x</sub> catalysts

Chaoli Tong, Jiachang Zuo, Danlu Wen, Weikun Chen, Linmin Ye, Youzhu Yuan (✉)

State Key Laboratory of Physical Chemistry of Solid Surfaces, National Engineering  
Laboratory for Green Chemical Productions of Alcohols-Ethers-Esters, *iChEM*, College of  
Chemistry and Chemical Engineering, Xiamen University, Xiamen 361005, China

E-mail: yzyuan@xmu.edu.cn

**Table S1.** Textural properties of H-MOR and CuCeO<sub>x</sub>/H-MOR catalyst.

Catalyst	$S_{\text{BET}}$ /m <sup>2</sup> g <sup>-1</sup>	$S_{\text{micropore}}$ /m <sup>2</sup> g <sup>-1</sup>	$V_{\text{pore}}$ /mL g <sup>-1</sup>	$V_{\text{micropore}}$ /mL g <sup>-1</sup>	$D_{\text{pore}}$ /nm
H-MOR	355	334	0.17	0.14	1.9
CuCeO <sub>x</sub> /H-MOR	304	172	0.28	0.07	3.7

**Table S2.** The radius<sup>[1]</sup> of element Cu and Ce.

Element	Radius /nm	Element	Radius /nm
Cu	0.128	Ce	0.183
Cu <sup>2+</sup>	0.073	Ce <sup>3+</sup>	0.183

[1] Z. H. Li. Data manual of element properties [M]. Hebei People's publishing house, 1985.

**Table S3.** Element content in smooth region of CuCeO<sub>x</sub>/H-MOR catalyst before calcination.

Element symbol	Atomic conc. /%
O	66.31
Si	28.06
Al	2.85
Cu	1.47
Ce	1.32

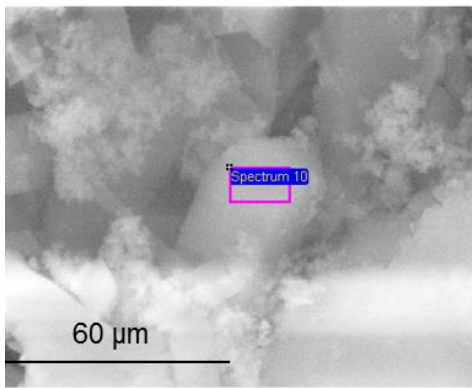


**Table S4.** Element content in smooth region of CuCeO<sub>x</sub>/H-MOR catalyst after calcination at 500 °C for 4 h.

Element symbol	Atomic conc. /%
O	62.84
Si	31.34
Al	2.91
Cu	1.94
Ce	0.98

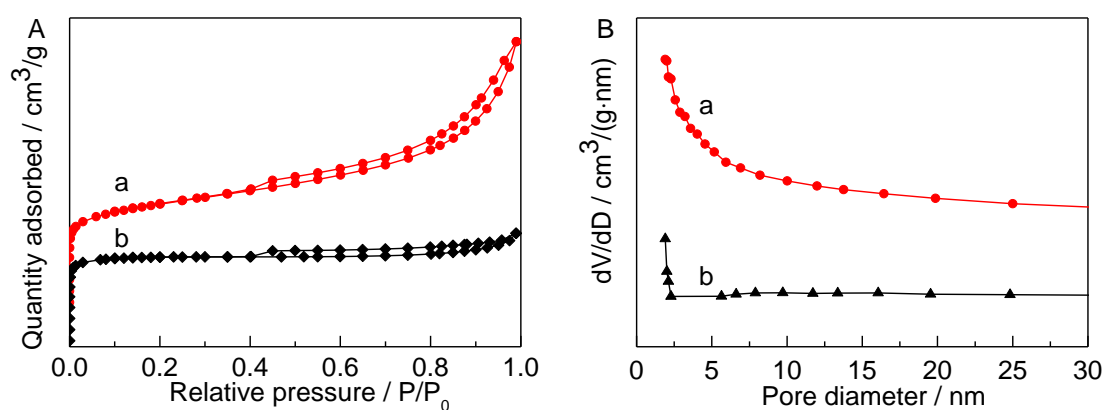
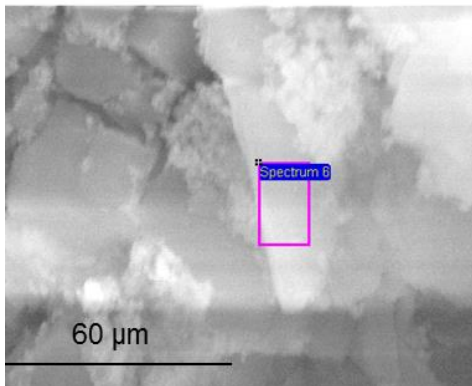


**Fig. S1** (A) Ar adsorption–desorption isotherms and (B) pore-size distributions of (a) CuCeO<sub>x</sub>/H-MOR and (b) H-MOR catalyst.

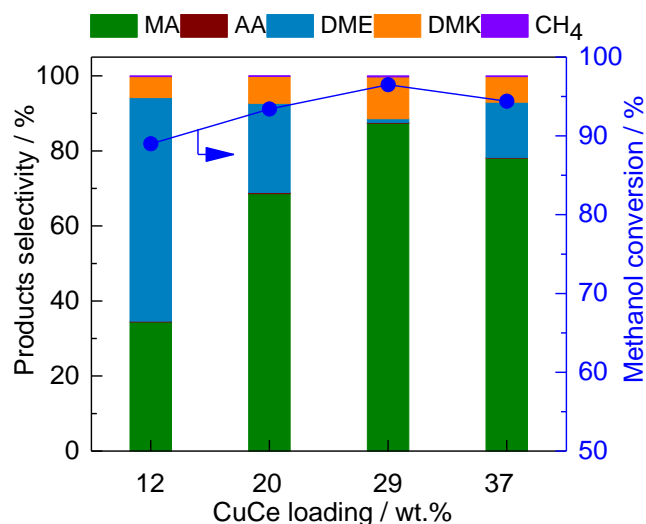


**Fig. S2.** Effect of the metal loadings on CuCe catalyst for methanol heterogeneous carbonylation reaction. Reaction conditions:  $T = 200\text{ }^{\circ}\text{C}$ ,  $P_{\text{CO}} = 1.0\text{ MPa}$ ,  $\text{CH}_3\text{OH}/\text{CO} = 2.15$  mol%,  $F = 10\text{ mL min}^{-1}$ , time on stream = 3 h.

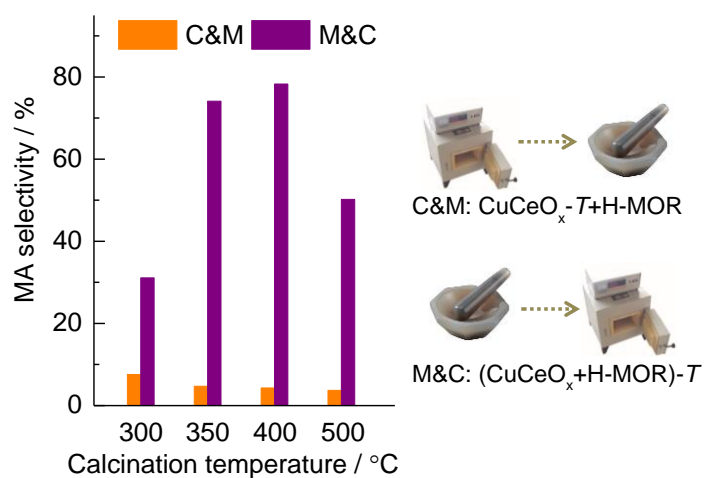


**Fig. S3** MA selectivity of two comparative experiments at different calcination temperatures.

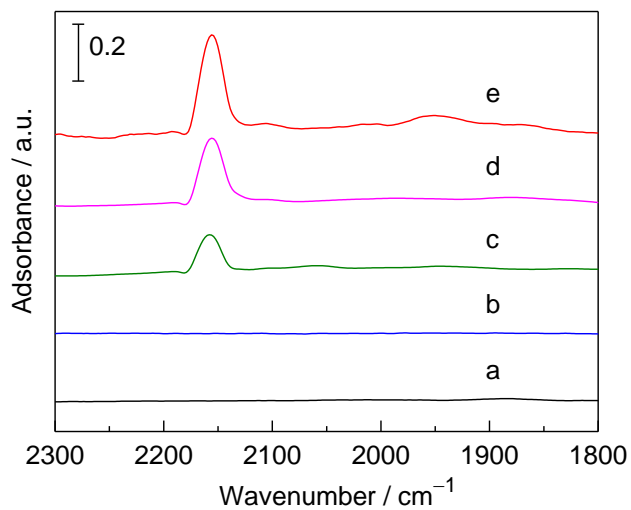


**Fig. S4** FT-IR spectra of the chemisorbed CO on as-reduced catalyst after evacuation for 25 min (a) H-MOR, (b) CuCeO<sub>x</sub>, (c) H-MOR+CuCeO<sub>x</sub>, (d) Cu-H-MOR+CuCeO<sub>x</sub>, and (e) CuCeO<sub>x</sub>/H-MOR.

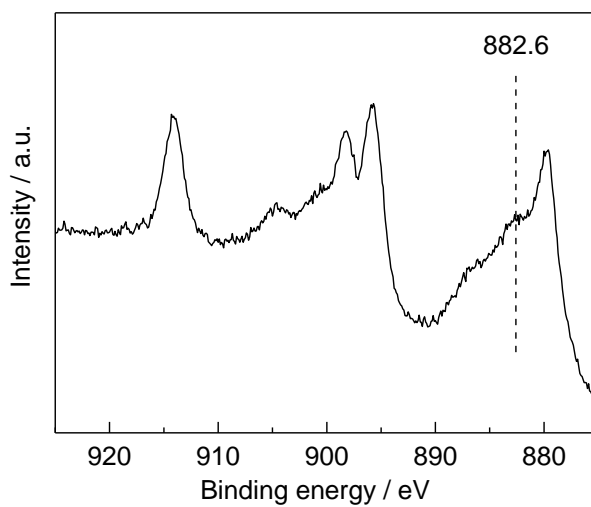


**Fig. S5** Ce 3d XPS of in situ reduced CuCeO<sub>x</sub>/H-MOR.

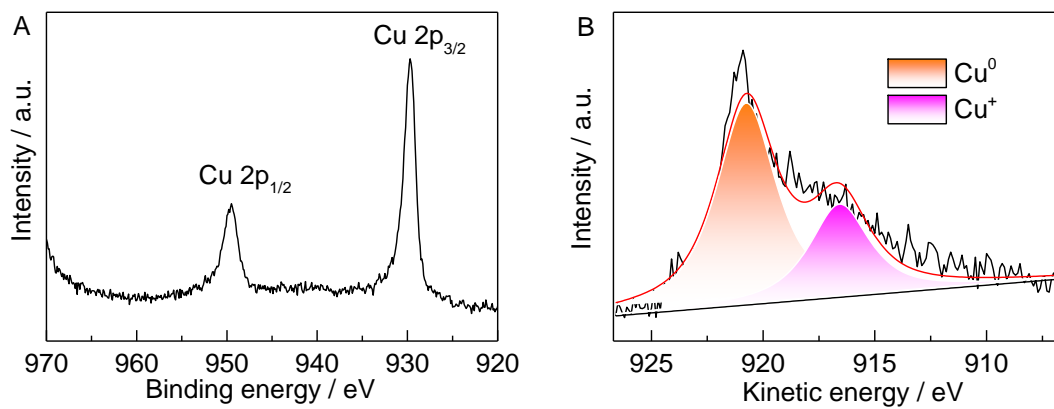


**Fig. S6** (A) Cu 2p XPS and (B) Cu LMM AES of in situ reduced CuCeO<sub>x</sub>/H-MOR.

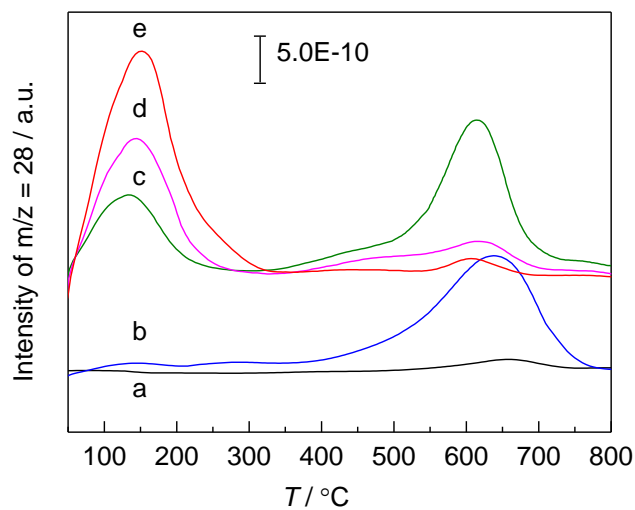


**Fig. S7** CO-TPD profiles of different catalysts (a) H-MOR, (b) CuCeO<sub>x</sub>, (c) H-MOR+CuCeO<sub>x</sub>, (d) Cu-H-MOR+CuCeO<sub>x</sub>, and (e) CuCeO<sub>x</sub>/H-MOR.

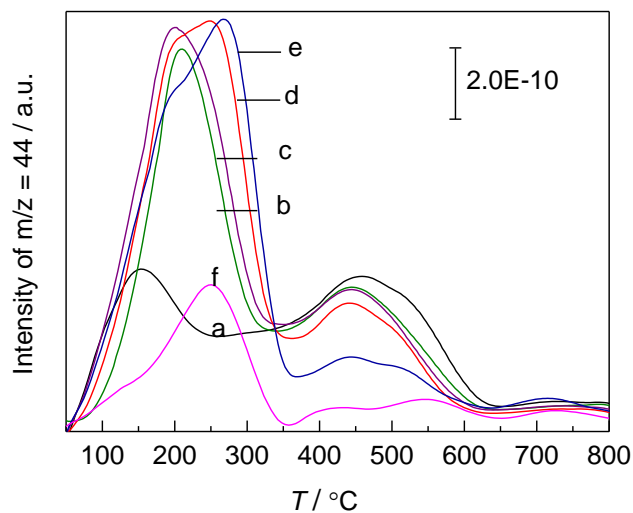


**Fig. S8** CO<sub>2</sub> signal from CO-TPD profiles of CuCeO<sub>x</sub>/H-MOR catalyst treated in air by different calcination temperatures: (a) 300 °C, (b) 350 °C, (c) 400 °C, (d) 500 °C, (e) 600 °C, and (f) 700 °C. Cu: 9.2 wt.%, Ce: 19.6 wt.%.

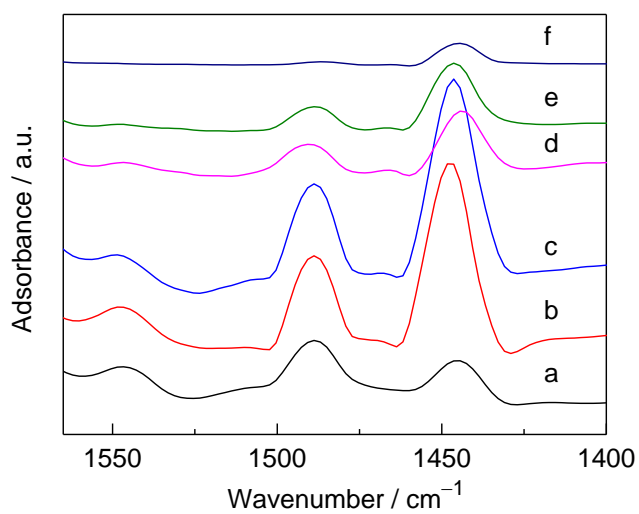


**Fig. S9** Pyridine-adsorbed FT-IR spectra of CuCeO<sub>x</sub>/H-MOR catalyst treated by different calcination temperature (a) 300 °C, (b) 350 °C, (c) 400 °C, (d) 500 °C, (e) 600 °C, and (f) 700 °C (1540 cm<sup>-1</sup> = B acid sites, 1450 cm<sup>-1</sup> = L acid sites).

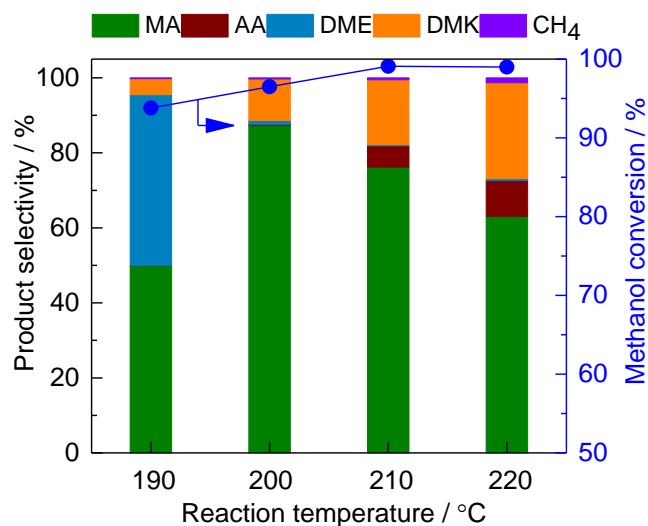


**Fig. S10** Catalytic performance of CuCeO<sub>x</sub>/H-MOR catalyst with different reaction temperatures for heterogeneous methanol carbonylation. Reaction conditions:  $P_{\text{CO}} = 1.0$  MPa, CH<sub>3</sub>OH/CO = 2.15 mol%,  $F = 10$  mL min<sup>-1</sup>, time on stream = 3 h.

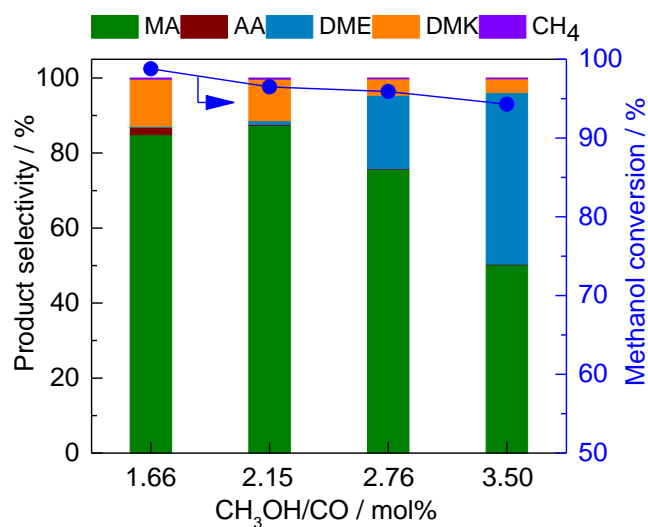


**Fig. S11** Catalytic performance of CuCeO<sub>x</sub>/H-MOR catalyst with different CH<sub>3</sub>OH/CO ratios for heterogeneous methanol carbonylation. Reaction conditions:  $T = 200$  °C,  $P_{\text{CO}} = 1.0$  MPa,  $F = 10$  mL min<sup>-1</sup>, time on stream = 3 h.

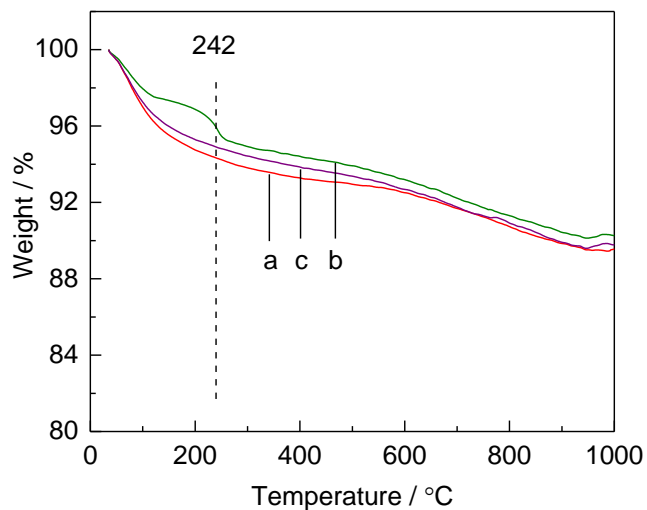


**Fig. S12** TG curves of (a) as-calcined  $\text{CuCeO}_x/\text{H-MOR}$ , (b) spent  $\text{CuCeO}_x/\text{H-MOR}$ , and (c) regenerated  $\text{CuCeO}_x/\text{H-MOR}$  by burning coke.

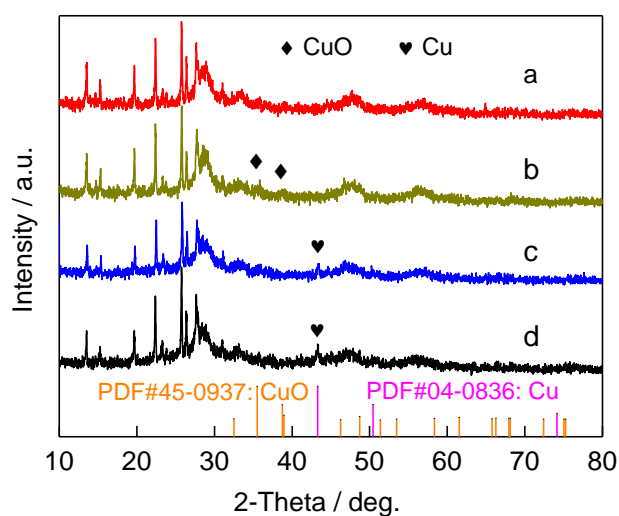


**Fig. S13** XRD patterns of (a) as-calcined  $\text{CuCeO}_x/\text{H-MOR}$ , (b) regenerated  $\text{CuCeO}_x/\text{H-MOR}$  by burning coke, (c) as-reduced  $\text{CuCeO}_x/\text{H-MOR}$  by 5%  $\text{H}_2/\text{Ar}$ , and (d) spent  $\text{CuCeO}_x/\text{H-MOR}$ .

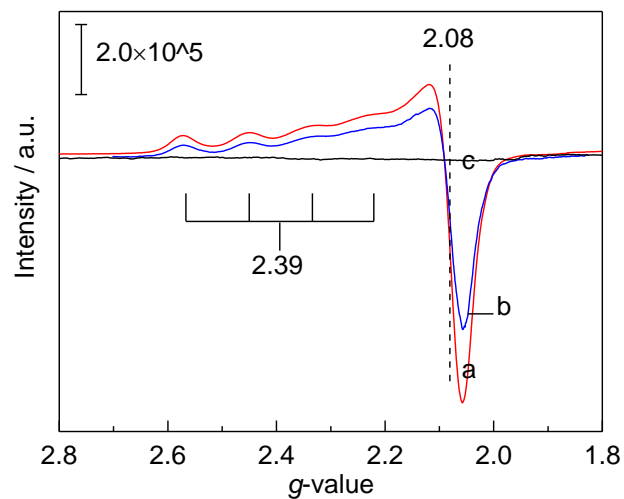


**Fig. 14** ESR profiles of (a) as-calcined  $\text{CuCeO}_x/\text{H-MOR}$ , (b) regenerated  $\text{CuCeO}_x/\text{H-MOR}$  by burning coke, and (c)  $\text{CuCeO}_x$ .